Estimating forest productivity in the eastern Siskiyou Mountains of southwestern Oregon using a satellite driven process model, 3-PGS

N.C. Coops and R.H. Waring

Abstract: The 3-PGS (physiological principles for predicting growth using satellite data) model generates monthly estimates of transpiration, photosynthesis, and net primary production (NPP), the latter derived as a fixed proportion (0.47) of gross photosynthesis. To assess the reliability of a simplified process model (3-PGS) to predict the productive capacity of coniferous forest across diverse landscapes in southwestern Oregon, we first used a geographic information system to display and manipulate basic data. This involved the following steps: (*i*) extrapolate monthly mean weather data to reflect topographic variation; (*ii*) transform monthly temperature extremes to spatial resolution of 4 ha and estimate incoming solar radiation, subfreezing days per month, daytime vapor pressure deficits, and mean temperatures; (*iii*) convert statewide soil survey maps into topographically adjusted estimates of soil fertility and water storage capacity (θ); and (*iv*) acquire satellite-derived estimates of the faction of light intercepted by vegetation during midsummer. Model predictions of soil water availability during summer months compared well with those reported from published measurements of predawn water potentials at three contrasting sites and with measurements acquired at the end of seasonal drought at 18 sites (r^2 = 0.78 with mean monthly modeled drought index; r^2 = 0.57 with seasonal modeled drought index). Similarly, seasonal shifts in the relative importance of various climatic and edaphic variables closely matched those defined in previously published studies. Finally, model predictions of maximum annual aboveground growth were compared with those derived from forestry yield tables based on height–age relationships with a resulting r^2 of 0.76, and a standard error of 1.2 $m^3 \cdot ha^{-1} \cdot year^{-1}$ (P < 0.01).

Résumé : Le modèle 3-PGS (principes physiologiques pour prédire la croissance à l'aide de données satellites) génère des estimés mensuels de la transpiration, de la photosynthèse et de la production primaire nette (PPN) qui est calculée sur la base d'une proportion fixe (0,47) de la photosynthèse brute. Les auteurs ont d'abord utilisé un système d'information géographique pour afficher et manipuler les données de base dans le but d'évaluer la fiabilité d'un modèle simplifié des processus (3-PGS) pour prédire la capacité de production de la forêt résineuse présente dans plusieurs paysages différents du sud-ouest de l'Oregon. Cette démarche comprenait les étapes suivantes : (*i*) extrapoler les données météorologiques mensuelles moyennes pour refléter les variations topographiques; (*ii*) transformer les extrêmes de température mensuelle à un niveau de résolution spatiale de quatre ha et estimer la radiation solaire incidente, le nombre de jours par mois où la température est sous le point de congélation, les déficits de pression de vapeur durant le jour et les températures moyennes; (*iii*) convertir les cartes d'inventaire des sols à l'échelle de l'État en estimés de la fertilité des sols et de la capacité de rétention d'eau (θ) ajustés en fonction de la topographie, et (*iv*) acquérir à partir de données satellitaires des estimés de la proportion de la lumière interceptée par la végétation au milieu de l'été. Les prédictions du modèle pour la disponibilité en eau du sol pendant les mois d'été se comparent avantageusement avec les valeurs rapportées dans la littérature sur la base de mesures du potentiel hydrique avant l'aube provenant de trois sites différents et avec les mesures prises au terme d'une sécheresse saisonnière dans 18 sites (r^2 = 0,78 avec la modélisation d'un indice mensuel moyen de sécheresse ; r^2 = 0,57 avec la modélisation d'un indice saisonnier de sécheresse). De la même façon, les variations saisonnières dans l'importance relative de diverses variables climatiques et édaphiques sont très semblables à celles qui ont été définies dans les études publiées antérieurement. Finalement, la croissance épigée annuelle maximale prédite par le modèle a été comparée à celle qui a été dérivée des tables de rendement en matière ligneuse basées sur les relations âge–hauteur. Cette comparaison a généré une valeur de r^2 de 0,76 et un écart-type de 1,2 $m^3 \cdot ha^{-1} \cdot an^{-1}$ (P < 0,01).

[Traduit par la Rédaction]

Introduction

The Pacific Northwest region of the United States contains some of the most productive forests in North America (Whittaker 1961). In this region, there is an increasing demand for geographically registered information to provide a sound basis for land-use planning. To meet this demand, two major properties of forested landscape need to be deter-

Received November 25, 1999. Accepted October 16, 2000. Published on the NRC Research Press website on January 8, 2001.

N.C. Coops.[1] CSIRO Forestry and Forest Products, Private Bag 10, Clayton South 3169, Melbourne, Australia.
R.H. Waring. Oregon State University, College of Forestry, Corvallis, OR 97331, U.S.A.

[1]Corresponding author. e-mail: n.coops@ffp.csiro.au

 DOI:10.1139/cjfr-31-1-143

mined: the potential productivity and current forest growth rates. The past two decades have seen considerable progress in developing process-based models to predict current and potential forest productivity (Landsberg and Coops 1999). These process-based models aim to simulate the growth of stands in terms of the underlying physiological processes and the way stands are affected by the physical conditions to which trees are subject and with which they interact. Process-based models have the potential to be far more flexible than empirical relationships and can be used in a heuristic sense to evaluate the consequences of change and the likely effects of stimuli (Landsberg and Gower 1997). In general, these models have proved useful for integrating different processes and scales of knowledge (Landsberg and Gower 1997), for honing research hypotheses, and for making broad predictions of relative productivity regionally or under different environmental change scenarios (Landsberg et al. 2001).

Models

Landsberg and Waring (1997) developed a simple process-based forest growth model called 3-PG[2] (physiological principles for predicting growth) based on a number of established biophysical relationships and constants. The model requires few parameters, and these are easily derived from literature or from field measurements. The model has a monthly time step and requires mean daily short-wave incoming radiation, mean vapor pressure deficits, temperature extremes, total monthly rainfall, and estimates of soil water storage capacity and fertility.

Absorbed photosynthetically active radiation (ϕ_{pa}) is estimated from global solar radiation derived, if necessary, from an established empirical relationship based on average maximum and minimum temperatures (Coops et al. 2000*b*). The utilized portion of ϕ_{pa} (ϕ_{pau}) is obtained by reducing ϕ_{pa} by an amount determined by a series of modifiers (Landsberg and Gower 1997) derived from constraints imposed by (*i*) stomatal closure, caused by high day-time atmospheric vapor pressure deficits (D) (see Landsberg and Waring 1997); (*ii*) soil water balance, which is the difference between total monthly rainfall, plus available soil water stored from the previous month, and transpiration, calculated using the Penman–Monteith equation with canopy conductance modified by leaf area index (L) of the forest and constrained by monthly estimates of D's (reaching a maximum value of $0.02\ \mathrm{m \cdot s^{-1}}$); (*iii*) the effects of sub-freezing temperatures (<0°C) using a frost modifier calculated from the number of frost days per month; and (*iv*) a temperature quadratic function, which varies between zero and unity to reduce the photosynthetic capacity when monthly mean temperatures are suboptimal (J.J. Landsberg, R.H. Waring, and N.C. Coops, submitted). The temperature optimum for coastal Douglas-fir (*Pseudotsuga menziesii* (Mirb.) Franco) is about 20°C, with a minimum threshold of 0°C and a maximum of 40°C (Lewis et al. 1999). The modifiers take values between 0 (system "shutdown") and 1 (no constraint) (see Landsberg 1986; Runyon et al. 1994). Gross primary production (P_G) is calculated by multiplying ϕ_{pa} by a canopy quantum efficiency coefficient (α_c). A major simplification in the 3-PG model is that it does not require calculation of respiration or root turnover but, rather, assumes that total net primary production (P_N) in temperate forests is approximately a fixed fraction (0.47 ± 0.04) of P_G (Landsberg and Waring 1997; Waring et al. 1998; Law et al. 1999). The model partitions P_N into root and aboveground biomass. The fraction of total P_N allocated to root growth increases from 0.2 to 0.6 as the ratio ϕ_{pau}/ϕ_{pa} decreases from 1.0 to 0.2.

The 3-PG model has been applied to forest environments in Australia and New Zealand (Landsberg and Waring 1997), South America, South Africa, the United Kingdom (Waring 2000), and North America (Law et al. 1999; Landsberg et al. 2001; Coops et al. 2000*a*).

Coops et al. (1998*a*) modified the 3-PG model to allow it to be driven with satellite observations (3-PGS) to assess seasonal changes in the capacity of the vegetative canopy to intercept radiation. In 3-PGS, the fraction of photosythetically active radiation absorbed by the forest canopies (fPAR) is estimated from a satellite-derived index, based on the normalized difference between reflectances measured in the near-infrared and red wavelengths, termed the normalized difference vegetation index (NDVI). This spectral vegetation index has been shown, both empirically and theoretically, to be related to the fPAR absorbed by vegetation canopies (Kumar and Monteith 1982; Sellers 1985, 1987; Goward et al. 1994).

Coops et al. (1998*a*) utilized 3-PGS to predict aboveground net primary production (NPP_A) at eight contrasting forested sites in Australia and New Zealand and compared them with estimated NPP_A derived from field data. In 3-PGS the biomass partitioning between foliage and stems, as well as leaf litter fall, root decomposition, and self-thinning routines, present in the 3-PG model are not implemented. For these reasons the analysis was restricted to comparisons of NPP_A. Likewise, data from the coarse-scale U.S. National Oceanic and Atmospheric Administration (NOAA) advanced very high resolution radiometer (AVHRR) instrument was used making the scale of analysis broad (8 × 8 km), reducing the requirement (or possibility) for recognising species, size classes, individual plot treatments, or annual rates of mortality. In that study there was a linear relation between NPP_A predicted by the model and on the ground estimates of wood production (usually >75% of NPP_A) for (potentially) fully stocked, rapidly growing stands (r^2 = 0.82). The analysis also provided an assessment of the relative importance of climatic variables upon production.

Additional research by Coops et al. (1998*b*) demonstrated that the 3-PGS model could be utilized in management applications by linking 1-km^2 NOAA AVHRR data with Landsat Multi-Spectral Scanner (MSS) data to incorporate "snapshots" of the forest using fine-scale (80 m) spatial resolution data obtained at specific time intervals. These higher resolution remotely sensed data provided the possibility to include a number of additional key spatial variables not available at the 1-km scale, specifically, forest age-classes, soil fertility, and water holding capacity. NPP_A predicted by 3-PGS in a *Pinus radiata* D. Don plantation in southern New South Wales, Australia, was in excellent agreement (r^2 =

[2] Additional information on this research and the 3-PG model is available at <http://www.fsl.orst.edu/bevr/ and mirrored at http://www.ffp.csiro.au/>

Table 1. Stand descriptions.

Plot	Elevation (m)	Slope (%)	Aspect	Parent material	Dominant vegetation
1	1490	25	W	Granite	White fir, ponderosa pine, Douglas-fir
2	1675	60	WNW	Granite	White fir, Douglas-fir
3	780	45	N	Granite	Douglas-fir, black oak, ponderosa pine
4	1920	65	SE	Ultrabasic	Jeffrey pine, incense-cedar, western white pine
5	1710	65	SE	Ultrabasic	Jeffrey pine, incense-cedar
6	2040	35	NNE	Granite	Mountain hemlock, Shasta red fir
7	1920	20	N	Granite	Shasta red fir
8	1280	40	SW	Granite	Ponderosa pine, Douglas-fir
9	1550	55	NNW	Meta-volcanic	White fir, sugar pine, Shasta red fir
10	1740	55	N	Meta-volcanic	Brewer spruce, Shasta red fir, mountain hemlock
11	1370	35	SW	Granite	Ponderosa pine, sugar pine, white fir, Douglas-fir
17	1830	10	E	Meta-volcanic	Shasta red fir
18	2135	30	NE	Granite	Mountain hemlock
20	760	70	NNW	Mica schist	Douglas-fir, Pacific yew
21	550	75	N	Meta-volcanic	Douglas-fir, black oak, Oregon white oak
22	1460	50	N	Meta-sedimentary	Douglas-fir, white fir
23	1400	10	N	Granite	Engelmann spruce, Douglas-fir, white fir
25	1740	5	SE	Ultrabasic	Jeffrey pine, white fir, incense-cedar, Douglas-fir

0.84) with measured actual forest productivity. By incorporating both fine- and coarse-resolution data the effects of thinning and other disturbances could be taken into account, greatly improving estimates of actual growth.

In this paper, we apply the 3-PGS model across southwestern Oregon to make broad-scale predictions using extrapolations of climatic data and 12 months of AVHRR, 1-km, NDVI imagery. Two comparisons were undertaken; firstly, 3-PGS soil water balance predictions were compared with previously reported monthly and seasonal water stress patterns; and secondly, 3-PGS growth predictions were compared with yield table estimates derived from measurements of site index (reference to height at 100 years).

Methods

Study area

The Siskiyou Mountains, which extend on both sides of the California–Oregon border, are the most northern portions in the Klamath Mountains Geological Province (Irwin 1966). Across the Siskiyous, from the Coast Range to the Cascades, a steep climatic gradient exists with annual precipitation decreasing from over 250 cm to less than 50 cm. Superimposed on the climatic gradient is extensive geological diversity; consequently, the Siskiyou Mountains are an area of significance to the evolution and migration of western forest flora (Whittaker 1961). This region of southwestern Oregon is atypical of the rest of the Douglas-fir region in the Pacific Northwest. The vegetation, soils, and disturbance history from gold mining, fire, and logging is complex, also the flora in the area is evolutionarily more closely related to that in China and the Appalachian Mountains of the southeastern United States than elsewhere in the West.

The Siskiyou Mountains are much older than the surrounding mountains. Parent materials represent a broad array of chemical compositions from acidic granites to ultrabasic peridotites, as well as materials of metamorphic and sedimentary origins. The most fertile soils are derived from a graphite mica schist and the most infertile soils are derived from peridotite and its metamorphic equivalent, serpentine (Waring and Youngberg 1972).

The region's vegetation has been classified in relation to its floristic variation and growth along physiologically defined gradients of moisture, temperature, light, and soil fertility (Waring 1969; Atzet and Waring 1970; Waring and Youngberg 1972; Waring et al. 1972; Reed and Waring 1974; Waring et al. 1975). This body of work provides a good foundation for interpreting predictions derived from the 3-PGS model.

Existing plot data

As part of a larger vegetation survey program in Oregon and California, Waring (1969) established 19 plots whose data were the basis of this comparison. At each of the 19 stands, a series of measurements were acquired between 1965 and 1975 on air and soil temperature, radiation, humidity, vapor pressure deficit, soil moisture, and soil fertility. (Refer to references cited in the last paragraph.) To serve as references, all physiological responses were measured on two widely distributed conifers, Douglas-fir and Shasta red fir (*Abies magnifica* var. *shastensis* Lemm.). Measurements included phenology, plant water potential, stomatal resistance, and foliar nutrition as well as standard forestry inventory data including stand height and age.

In 1999, we revisited all 19 plots and noted that all but one (plot 19) were intact with the original trees still at maximum height indicating that site index values would not have changed since reported in Waring et al. (1972). As a result, the data set was reduced to 18 plots. (See Table 1 for brief stand descriptions.)

During the 1966 growing season, plant water potential was measured with a pressure chamber (Scholander et al. 1965; Waring and Cleary 1967). Measurements were taken at monthly intervals from April through September at all 18 plots. Most of the published work reports only minimum plant water potentials measured near the end of seasonal drought; however, seasonal trends were presented for three major vegetation types: oak, pine, and Shasta red fir (Waring et al. 1972). These patterns were consistent from year to year and allow one to infer seasonal changes in the relative availability of water to 1–2 m tall trees at all sites. At the peak of drought in September, predawn water potentials ranged from –0.5 MPa on sites with deep soils, or where deep winter snowpack accumulated or where seepage occurs to –2.5 MPa on lower elevation sites with shallow or extremely sandy or rocky soils (Waring and Cleary 1967; Waring 1969).

Waring (1969) estimated site index by measuring height and age of dominant trees at all the plots. On infertile ultrabasic soils, site index overestimates stand productivity, because although individual trees reach moderate height, the density of trees remains low (Waring 1970; Waring and Youngberg 1972; Reed and Waring 1974). From estimates of site index, maximum volume growth increments for Douglas-fir were estimated from standard yield tables (McArdle 1961). We selected Douglas-fir as a reference species, because it occurred on most of the plots and its growth correlates well with other species. Sitka spruce (*Picea sitchensis* (Bong.) Carr.) yields are 20% higher, and those of ponderosa pine (*Pinus ponderosa* Dougl. ex Laws.) are 20% lower, for equivalent site indices in southwestern Oregon (Waring 1970; Hann and Scrivani 1987).

Requirements for 3-PGS model

Climate

As site-index values reflect long-term climate and soil properties at each plot location, we used long-term climatic records rather than those acquired in 1960s or in 1995 when satellite imagery was obtained (see below). Mean monthly minimum and maximum temperature and precipitation surfaces of the region were acquired with the PRISM (parameter-elevation regressions on independent slopes model) software, which is an expert system that uses 30 years of meteorological station data and a digital elevation model (DEM) to generate gridded estimates of mean climate parameters (Daly et al. 1994). PRISM was specifically developed to predict climate variables in Oregon; thus, the effects of terrain on climate played a central role in the model's conceptual framework.

Radiation

Monthly estimates of total incoming short-wave radiation were calculated using a modeling approach detailed in Coops et al. (2000*b*) that allows solar radiation to be predicted across landscapes by first calculating potential radiation at the top of the atmosphere and then reducing that value based on the clarity (transmissivity) of the atmosphere as a function of elevation (Goldberg et al. 1979; Bristow and Campbell 1984; Hungerford et al. 1989). Bristow and Campbell (1984) developed a methodology that correlated changes in the atmospheric transmissivity with temperature extremes recorded daily and summarized monthly. With a DEM we corrected for the effect of slope, aspect, and elevation on incoming radiation as well as for variations in the fraction of diffuse and direct solar beam radiation (Garnier and Ohmura 1968; Buffo et al. 1972; Swift 1976; Hungerford et al. 1989). Comparison with measured radiation data demonstrated that the modeling approach predicted mean monthly incoming radiation with 93–99% accuracy on flat ground and under conditions of sloping terrain, mean monthly predictions of solar radiation accounted for >87% of the observed variation with mean errors <2 $MJ \cdot m^{-2} \cdot day^{-1}$ (Coops et al. 2000*b*)

Soil fertility

For regional-scale mapping and monitoring, the State Soil Geographic (STATSGO) data base is the most appropriate, because it has been compiled at a consistent scale (1 : 250 000) for all States (USDA 1991). STATSGO soil data are compiled from more detailed (SSURGO) soil survey maps and information on geology, topography, climate, and vegetation, supplemented by images from satellite remote sensing. Using the United States Geological Survey's (USGS) 1 : 250 000 scale, 1 × 2° quadrangle series as a map base, the soil data were digitized as line segments to comply with national guidelines and standards. Soil fertility was inferred from the STATSGO mineralogy classes that provided broad indications of the fertility of the major soil types in the region using a lookup table. These fertility classes were then scaled between 0 and 1.

The 3-PG originally maintained a constant α_c value originally equal to 0.03 mol C/mol photon (Landsberg and Waring 1997). Later studies by Battaglia and Sands (1997), however, have used much higher values (0.05 mol C/mol photon), and values from 0.04 to 0.055 mol C/mol photons have been reported from field measurements in Oregon on ponderosa pine and other conifers (Bond et al. 1999; Law et al. 2000). Additionally, based on the work of Coops et al. (2000*a*) and Waring (2000) from analysis of growth of Douglas-fir in the United States, and Sitka spruce plantations in the United Kingdom, α_c was set at a maximum of 0.07 mol C/mol photon. We thus allowed α_c to increase linearly from 0.035 to 0.07 mol C/mol photon (1.9–3.8 g $C \cdot MJ^{-1}$ ϕ_{pau}) over the range in fertility derived from the STATSGO data set.

Soil water holding capacity

For each STATSGO soil series, the depth of each soil horizon and its mean available soil water capacity (θ) was computed and summed for the entire profile to provide an estimate of θ for each polygon. In southwestern Oregon, drought-prone vegetation has the ability to extract some water even from underlying parent material (Zwieniecki and Newton 1994). The STATSGO vector coverage was converted to raster format with a spatial resolution (size of the cell) of 200 m (4 ha), approximately equivalent to a 1 : 250 000 scale. If an individual cell was composed of polygons representing more than one soil series, the dominant series was selected.

The mean values of θ from the STATSGO data set was modified to take into account fine-scale variation on a 200-m (4-ha) resolution DEM of the region. Zheng et al. (1996) proposed a simple model to modify θ that used the mean values of θ from the STATSGO data set and a DEM. The compound topographic index (CTI) was computed as a function of the contributing area upslope of a central cell and the slope at that central cell on the DEM (Moore et al. 1991) using the following formulae:

$$[1] \qquad \mathrm{CTI} = \ln\left(\frac{\alpha}{\tan(\beta)}\right)$$

where α is the specific catchment area expressed as square metres per unit width orthogonal to the flow direction and β is the slope angle. Higher values of CTI tend to be registered in the lower parts of watersheds and in convergent hollow areas associated with soils of low hydraulic conductivity or areas with more gentle slope than average (Beven and Wood 1983). Soil depth and silt and clay content tend to increase from ridge tops to the valley bottoms (Singer and Munns 1987). Coops (2000) describes the technique in additional detail and provides examples of the predictions compared with site data at a large number of sites in Oregon.

Shifting original plot locations

As the plot positions of the original 18 plots were not located using global positioning system (GPS) technology, a geographic information system (GIS) search technique was used to ensure that the terrain attributes recorded at each plot (such as elevation, slope, and aspect) corresponded to similar attributes extracted from the DEM thereby fine tuning the geographic location of each plot on the DEM and satellite imagery. An automated search procedure was developed whereby the initial location of each plot was, if necessary, shifted within specified bounds to give closer agreement with field estimates of aspect, slope, and elevation (Coops 2000). Specifically, the search routine sequentially identifies the nearest 200-m resolution cell within a search radius of five cells in which differences are within ±22.5° of aspect, ±20% of slope, and in closest possible agreement with elevation. Coops (2000) found, using this technique, the initial plot locations were shifted, on average, 78 m within the five-pixel search radius.

Satellite data

The interpretation of satellite imagery to produce vegetation attributes remains a challenging problem with a multitude of factors affecting the signal recorded by the satellite sensor. Despite these difficulties, there are some clear relationships between the

Fig. 1. The seasonal soil drought indices generated by 3-PGS from June through August from soil water modifiers is –0.47 for the oak type, –1.2 for the pine type, and –3.2 for the Shasta fir type, which correspond to measured minimum ψ_p of –3.0, –1.8, and –0.7 MPa, respectively (from Waring et al. 1972, Fig. 3).

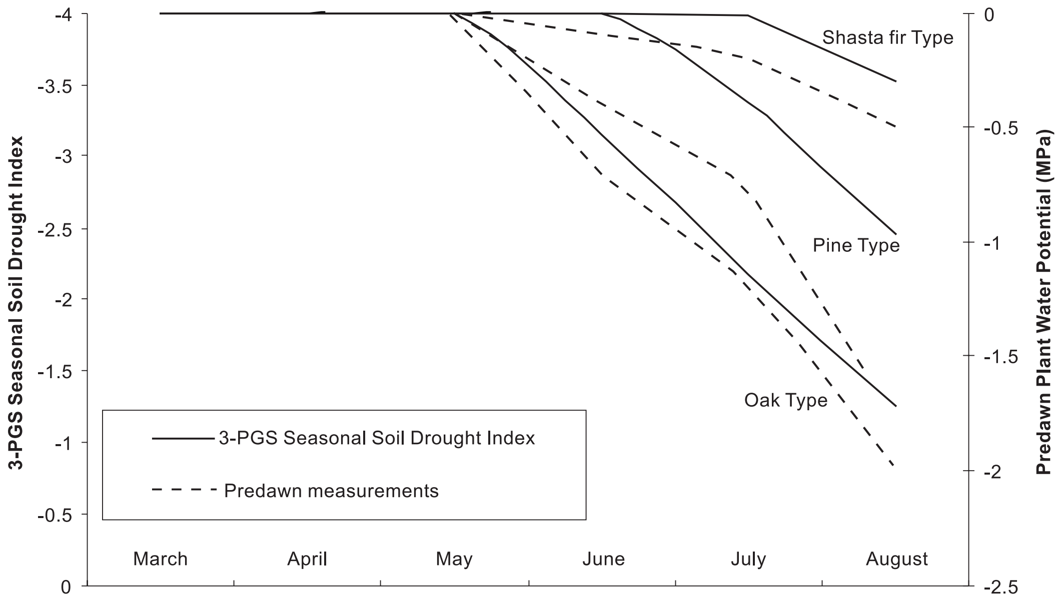

photosynthetic capacity of forest vegetation, regardless of species or age, and the spectral response of the vegetation in selected wavelengths, in particular, the visible and near-infrared part of the spectrum (Sellers 1985). The NDVI is a commonly applied index, and although a full explanation of the observed correlation between NDVI and canopy properties is still to be fully achieved, studies have shown that there is a linear, or near linear, relationship between NDVI and fPAR absorbed by vegetation canopies (Kumar and Monteith 1982; Sellers 1985, 1987; Goward et al. 1994). There are several limitations to such an inference but it appears that an estimate of the amount of PAR absorbed can be estimated from NDVI and knowledge of incoming solar radiation (Prince and Goward 1995).

One-kilometre monthly AVHRR NDVI imagery (Kidwell 1988) for 1995 was obtained and fPAR predicted from NDVI using equations developed by Goward et al. (1994). We then compared these predictions of fPAR at the OTTER reference sites (Peterson and Waring 1994) where ground-based measurements of fPAR were previously determined across a transect of vegetation (Runyon et al. 1994). We found it necessary to modify the slope of the relationship to match the previously published ground-based estimates of fPAR data, and a new equation was developed for this study.

The new equation is

[2] $$\text{Fraction of PAR absorbed} = 1.27I - 0.03$$

where I is the NDVI from the AVHRR data set.

3-PGS modelling of water stress

3-PGS models the soil water balance as the difference between total monthly transpiration and monthly precipitation. The model is initialized with available soil water content = maximum available water (θ, mm) in the soil profile (Landsberg and Gower 1997). The soil water balance is obtained as the difference between total monthly transpiration (mm), calculated using the Penman–Monteith equation and monthly precipitation. The moisture ratio (r_θ) for the stand is calculated as r_θ = (available soil water content + water balance (difference between total monthly transpiration and monthly precipitation))/(maximum available water). The water balance in any month will be negative if transpiration exceeds precipitation, and vice versa. If the numerator of the expression for r_θ exceeds θ, it is set to θ, i.e., the excess water is assumed to have run off or drained out of the system. If it is negative, $r_\theta = 0$.

The soil water modifier f_θ is calculated from the expression:

[3] $$f_\theta = \frac{1}{1+\left(\frac{1-r_\theta}{c_\theta}\right)^{n_\theta}}$$

where c_θ and the power n_θ take different values for each of four defined soil types (clay, clay loam, sandy loam, and sand) (Landsberg and Waring 1997).

Results

Relationship between soil water availability and predawn plant water potential

Predawn water potentials, measured when plants are not transpiring, are generally in close agreement with matric potentials in the vicinity of active roots (Lange et al. 1976; Waring and Running 1998). As the available soil water is depleted to below 60–80% of the maximum (the threshold is dependent on soil texture), predawn water potentials drop quickly until stomatal conductance is reduced to a minimum, where after all but cuticular transpiration is halted (Waring and Running 1998). In a drought-prone region such as southwestern Oregon, seasonal measurements of ψ_p show consistent seasonal trends and large differences amongst distinctive forest types.

We developed a seasonal soil drought index that was similar in sign and magnitude to measurements of ψ_p, starting in June with an initial value of –4 and added the monthly soil water modifiers through September. The seasonal drought index could thus vary from –4, indicating no depletion of available water, to 0, indicating no available water throughout the growing season.

Fig. 2. Modelled seasonal variation in the fraction of soil water available in the oak, pine, and Shasta fir sites (as in Fig. 1).

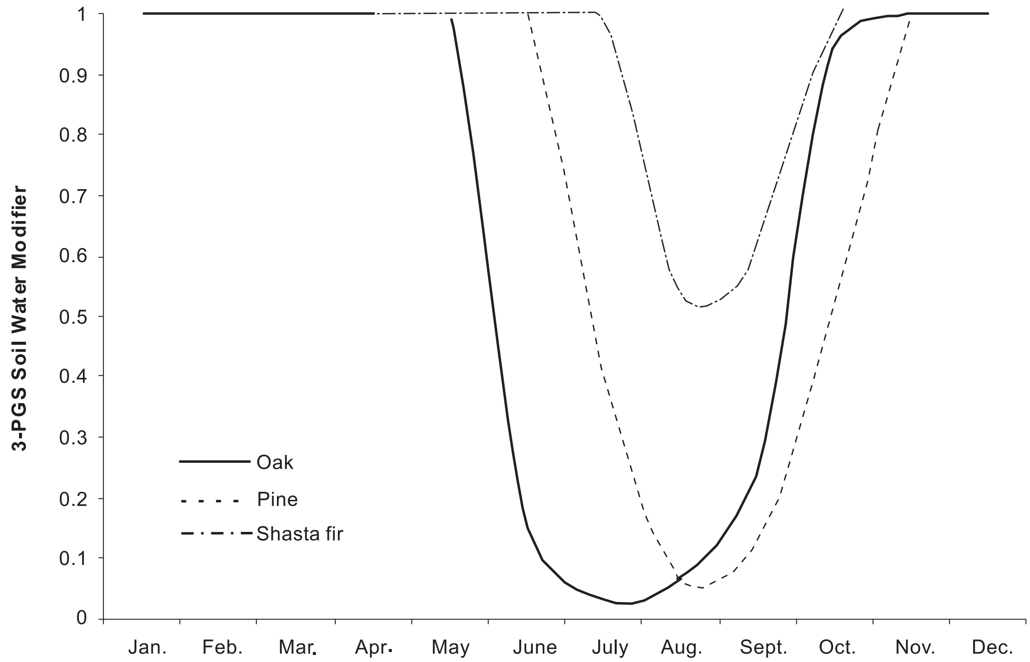

In Fig. 1, we present 3-PGS estimates of seasonal variation in the relative availability of soil water in reference to measured predawn water potentials for three distinctly different forest types: oak, pine, and Shasta red fir (Waring et al. 1972). The Shasta red fir type is restricted to moist sites where a heavy snow pack accumulates in winter and remains until July, while the California black oak (*Quercus kelloggii* Newb.) type grows where water stress is sufficient to bring about early cessation of cambial activity. In the Siskiyous Mountains, where effectively no rainfall occurs during the summer, ψ_p at the end of the growing season can be used to infer the relative availability of soil water to trees throughout the entire season. The seasonal drought index generated with 3-PGS compared well with minimum ψ_p values at the end of September: for oak, the seasonal drought index (SDI) was –0.47 with ψ_p = –3.0 MPa, for pine, SDI = –1.2 and ψ_p = –1.8 MPa, and for Shasta fir, SDI = –3.2 with ψ_p = –0.7 MPa.

The predicted seasonal variation in the fraction of available soil water for three forest types described previously in Fig. 1 is shown in Fig. 2. Through the winter months, the soil water supply remained at full capacity. As temperature and radiation increased in April and May, monthly water use by the vegetation increased, and the soil water supply was drawn down but to varying degrees.

At both the oak and pine types, the soil water supply was quickly depleted, resulting in major limitations after only 2 months of active forest growth. By late July, both of these types has exhausted, according to the model, most available water, whereas the Shasta fir type, situated on deep volcanic soils, had accessed only half of its available supply. As precipitation increased in late September and early October, the soil reservoir was predicted to be refilled.

Because ψ_p measurements were not taken at the same dates throughout the 1967 growing season (and are not reported in the literature) for all 18 plots, we compared minimum ψ_p values measured in the first week of September (Table 2) with the seasonal drought index generated from June through September (Fig. 3) (r^2 = 0.57). A linear relationship with the mean of the 3-PGS monthly soil water modifiers for the same months increased the predictive power from 57 to 78%. Three of the stands (17, 6, and 7) showed little ψ_p stress with values remaining above –0.5 MPa. 3-PGS predicted seasonal drought indices for these stands that ranged between –2.0 to –3.2. At the other extreme, two plots (3 and 21) experienced minimum ψ_p less than –2.5 MPa. These plots were predicted by 3-PGS to have soil water modifiers as low as 0.08 in late September, representing a 92% constraint on photosynthesis.

A complete listing of the estimates of maximum available soil water (θ) for all 18 plots is presented in Table 2, along with calculations of the mean monthly and seasonal drought indices, and published values of ψ_p (Waring et al. 1972). Although the water storage estimates were based solely on the DEM and soil series data, the predictions seems reasonable. In addition, Table 2 lists *L* for each of the plots based on fPAR derived from the AVHRR NDVI data, which was inverted by applying the Beer–Lambert law, to predict *L* (Gower et al. 1999). It should be noted that our *L* predictions differ from the original values published by Waring et al. (1978). Those earlier published values were for total surface area, which is approximately 2.5 larger times than projected surface area reported here. The original values should also be reduced by an additional 50% as they were found to be bias toward larger trees (Marshall and Waring 1986).

Climatic stand stress

A more detailed analysis of the environmental constraints on photosynthesis (and growth) is presented in Fig. 4 for the three forest types. In the winter months, the major restriction on photosynthesis is temperature, which is well below the optimum temperature for Douglas-fir as defined in the 3-PGS model. Frost, which is an additional modifier in 3-PGS (see Landsberg and Waring (1997) for explanation), is also a significant limitation to photosynthesis in the winter months.

Table 2. Predicted and measured water stress variables.

Plot	ψ_P (MPa)[a]	3-PGS mean monthly soil water modifer (June–Sept.)	3-PGS seasonal water stress index	θ (mm)[b]	L[c]
1	–1.53	0.48	–1.58	212	3.2
2	–1.53	0.40	–1.68	52	3.2
3	–2.54	0.08	–0.48	65	3.7
4	–1.53	0.43	–2.29	87	2.4
5	–1.81	0.39	–1.37	209	2.8
6	–0.52	0.50	–2.09	81	3.0
7	–0.52	0.40	–2.22	84	3.3
8	–2.03	0.17	–0.65	124	3.2
9	–1.62	0.37	–1.77	129	3.5
10	–1.91	0.37	–1.76	97	3.5
11	–1.53	0.28	–1.32	80	5.0
17	–0.52	0.84	–3.13	71	4.1
18	–1.91	0.47	–2.31	98	3.6
20	–1.62	0.38	–1.24	55	3.7
21	–2.54	0.05	–0.31	79	2.7
22	–1.28	0.32	–1.33	105	3.3
23	–1.28	0.41	–1.73	247	3.2
25	–1.53	0.40	–2.19	78	3.2

[a]$\psi_{p,}$ field-measured predawn water potential acquired in early September 1967 (Waring et al. 1972).
[b]θ, predicted mean available soil water capacity.
[c]L, leaf area index derived from Beer's Law using fPAR estimates from NDVI satellite-derived estimates acquired in 1995.

Fig. 3. The seasonal soil drought indices generated by 3-PGS from June through September from soil water modifiers is correlated (r^2 = 0.57) with early September 1967 measurements of ψ_p (MPa) made at 18 plots (refer to data in Table 2).

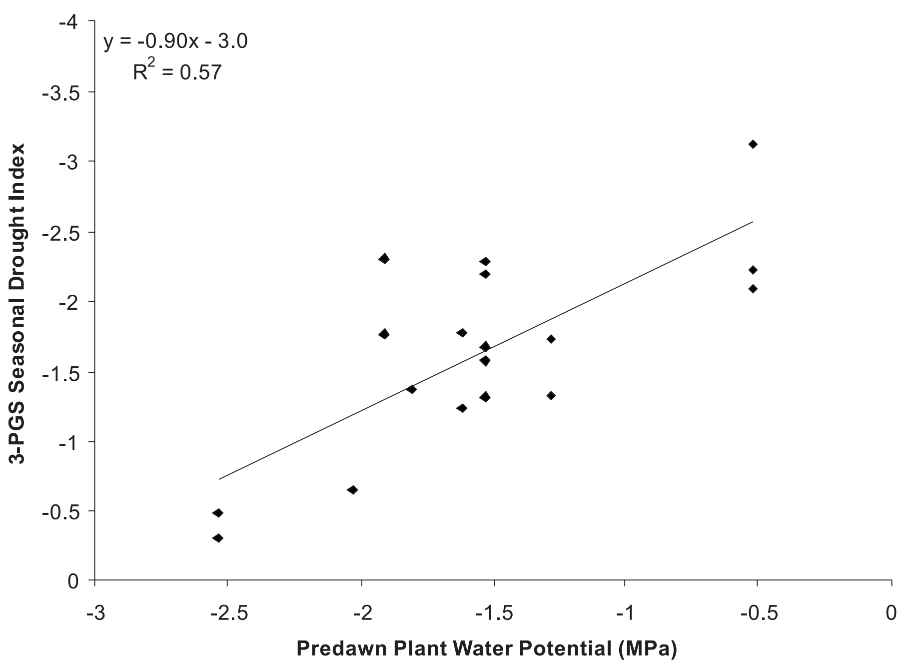

As the climate becomes warmer, restrictions from unfavorable temperatures were reduced along with the effect of frost. This improvement in temperature, however, was associated with increased limitations by D until drought began to exert a major influence during the summer. The lack of soil water stress at the Shasta fir site made D the most significant limitation to growth in July. Reductions in the availability of water, however, restricted growth somewhat in August and September even in the subalpine zone. As rain increased in the autumn, suboptimal temperatures together with frost became the dominant limitations, particularly in November and December.

The limitations of frost and temperature during the winter months extended over the entire region. But the higher elevation site, dominated by Shasta fir, was predicted to have photosynthesis and growth completely restricted, whereas the lower elevation pine and oak-dominated sites were able to continue to photosynthesize. The lower temperature during the summer at the Shasta fir site had a beneficial effect of lowering D. The lack of soil water storage at both the

Fig. 4. 3-PGS predicted modifiers for vapor pressure deficit (VPD), soil water stress, temperature, and frost for the three different forest types (Waring et al. 1972): (*a*) Shasta fir type, (*b*) pine type, and (*c*) oak type.

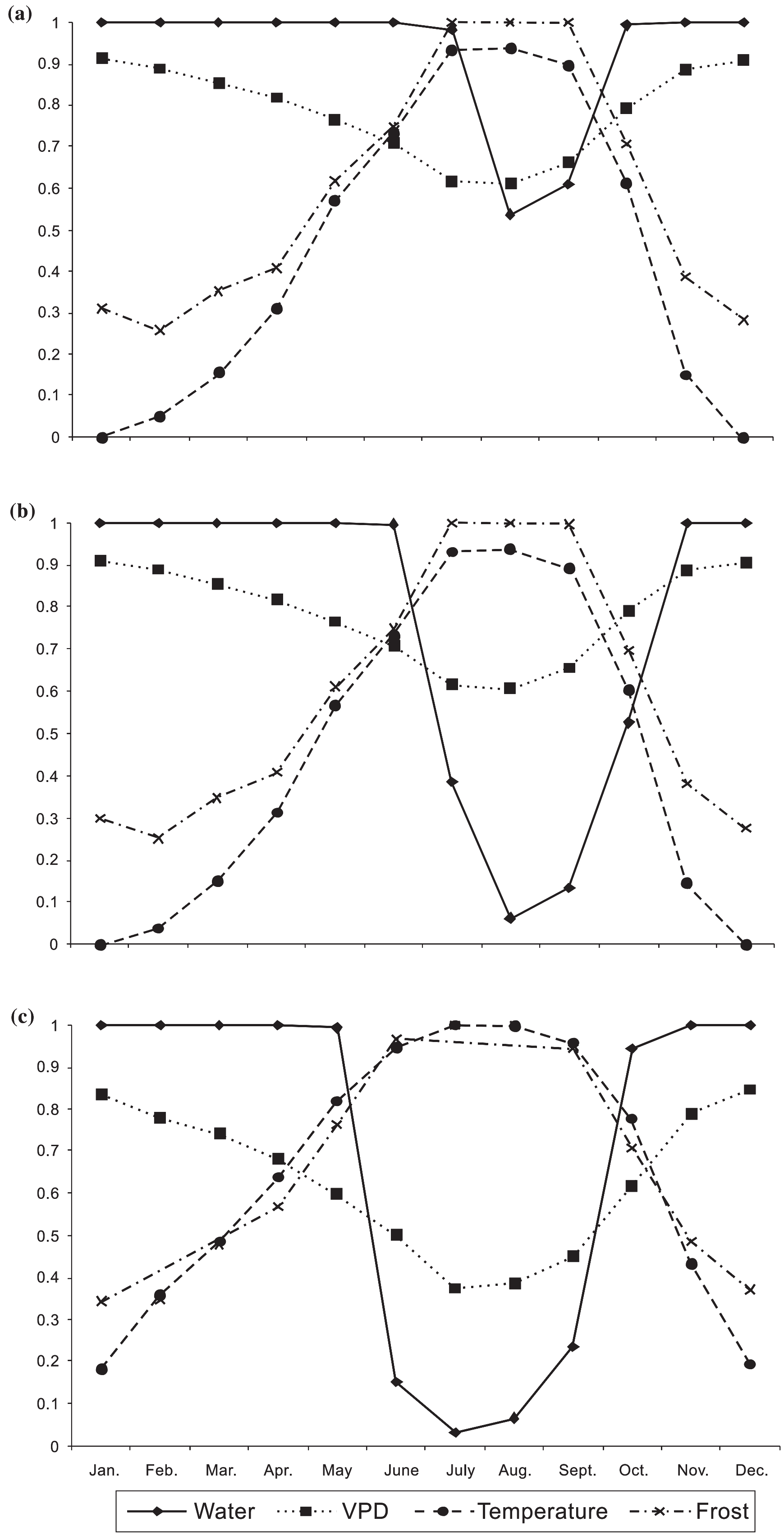

Fig. 5. Relationship between predicted and observed site index derived estimates of maximum volume growth ($m^3 \cdot ha^{-1} \cdot year^{-1}$) for the 18 stands, converted from biomass with wood density at 400 $kg \cdot m^{-3}$.

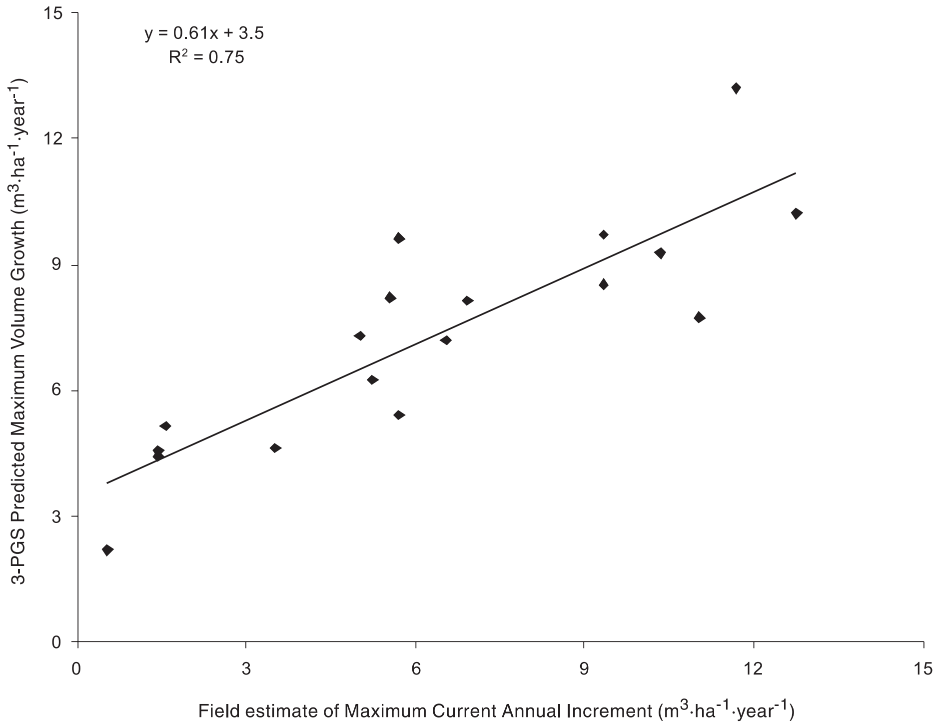

pine and oak sites in the summer months restrict growth, to around 10 and 40% of potential, respectively.

Forest stand maximum potential growth

Estimates of NPP_A derived for the 18 sites with 3-PGS are shown in Fig. 5. The simulations, using mean climatic data and l-km satellite imagery from 1995, indicate that the highest potential aboveground growth was at stands 11 and 17, mixed conifers and Shasta red fir stands, These stands receive above-average precipitation for the region and are situated on soils of above-average fertility. The lowest NPP_A recorded was at a Jeffrey pine (*Pinus jeffreyi* (Balfour)) stand situated on shallow, infertile soil derived from serpentine (Site 5). The overall relationship between predicted and estimated growth rates from yield tables ($m^3 \cdot ha^{-1} \cdot year^{-1}$) exhibited an r^2 of 0.76 with a standard error of 0.8 $m^3 \cdot ha^{-1} \cdot year^{-1}$, which was significant at $P < 0.01$.

The field-growth estimates used in this comparison were derived from measures of site index under the assumption that the forest stands were fully stocked with trees between the ages of 30 and 40 years when maximum productivity occurs. Underlying this assumption is the findings of Goward et al. (1985) and Franklin et al. (1997) that the peak NDVI values for a given area are similar, almost independent of the degree to which native vegetation has been disturbed. In fact, annual crops on non-irrigated agricultural lands often show maximum NDVI similar to that of native forests (Goward et al. 1985).

The relationship between the predicted NPP_A and estimated (as derived from field data) was generally good with an overall error of about ±25%. Biases in the relationship indicate that the site index estimated by the 3-PGS model were slightly higher in low-production areas and slightly lower in high-production areas than those estimated from field data. Figure 5 suggests that predicted yield values were generally less than the field estimates, which may reflect the fact that the yield tables used to estimate site index were developed from data collected in the Coast Range of Oregon, where stocking density and maximum leaf area indices are significantly higher than those observed in the Siskyous (Waring 1969).

Discussion

The benefits of ecosystem modeling include the capacity to extend traditionally point-based data acquired at scattered locations across landscapes and to incorporate generalized biophysical and physiological principles into scalable relationships. Models such as 3-PGS owe a debt to those who have previously developed full-fledged ecosystem models that combine water, carbon, and nutrient cycling. A few models like FOREST-BGC (Running and Coughlan 1988; Running and Gower 1991) and PnET (Aber and Federer 1992; Aber et al. 1995) have been successfully tested across regions. One of the most helpful aspects of these models is their ability to generate predictions of maximum *L* under any specified environment. In drought-prone areas, model simulations can quickly provide reasonable values of soil water storage capacity (Running 1994).

The 3-PGS model is much less comprehensive than other cited ecosystem simulation models as it does not include heterotrophic (microbial) respiration or mineral cycling (Ryan et al. 1997). It has, however, the advantage of not requiring the difficult calculation of autotrophic (plant) respiration through detailed carbon budgets by assuming a constant ratio of NPP/P_G for temperate forests of 0.47 (Waring et al. 1998).

Since this assumption was developed, additional information has been acquired for other temperate forests, indicating the original assumption of near constant ratio seems to hold, even for annual crops (Law et al. 1999; Malhi et al. 1999; Monje and Bugbee 1998).

In this paper, we make the assumption that over a 1 × 1 km area forest vegetation structure may be quite variable but fPAR inferred from satellite-derived measurements of NDVI would be similar, regardless of the present mix of vegetation. In the case of the Siskiyous, there is considerable topographic and geological variation within the mountainous regions. As a result, certain species and plant communities are restricted to specific microsites such as openings near rock outcrops, shaded seepage areas, alpine meadows, or chaparral vegetation types. There is an inherent scale limit on these predictions, with many of these 1 or 2 ha microsites not being discernable from the satellite imagery or their microclimate accurately represented on the DEM. The increased spatial and spectral resolution promised on the current generation of NASA's earth observing system (EOS) should provide improvements in recognizing variation in soils and vegetation (Running et al. 1994).

In this paper we make the assumption that mean climatic conditions predicted with the PRISM model were similar to climatic conditions at the sites in the 1960s when predawn water potentials and NPP_A data were acquired. Whilst any short-term climatic effects should not have a major effect on the prediction of site index, the predawn water potential measurements could be affected. Based on the observations of Waring (1969) and the results presented in this paper, we believe that using long-term weather data, along with more current satellite observations, do not compromise the interpretation of the relative importance of environmental variables at the 18 sites.

In drought-prone areas, such as the Siskiyou Mountains, it becomes important to obtain a good estimate of soil water holding capacity, which varies considerably with topography, soil development, and parent material. The technique utilized in this paper interprets fine spatial resolution patterns in topography to vary soil water holding capacity. Where springs bring water close to the surface, improved spatial resolution in satellite detection would be desirable. Our experience suggests, however, that adjusting survey plots to equivalent slopes, aspects, and elevations may still be more necessary. This involves using automated search procedures to shift the initial location of each plot within specified bounds to provide closer agreement with field measurements of aspect, slope, and soil water holding capacity. By relocating plots and by adjusting for topography we were able to make realistic estimates of soil water holding capacity. In regions where where evaporative demand is high, as in the eastern Siskiyous during the growing season, plant distribution is largely determined by the availability of water (Gholz 1982).

One of the most difficult variables to assess spatially over the region is soil fertility. Interpretations of the STATSGO data set are consistent with its broad level of geographic detail. The SSURGO data base would provide more detailed information, but this level of soil mapping is not yet available for most forested regions. On the other hand, the STATSGO soil data are often inadequate even for regional modeling, especially in mountainous areas. These inadequacies reflect variation present within 1-km^2 cells, as a result of insufficient sampling, and the difficulty of drawing boundaries between different mapping units (Mark and Csillag 1990; Burrough 1986). Nevertheless, the STATSGO data base provides the only available statewide mapping of soil attributes carried out in a consistent manner.

The current model implementation of 3-PGS is significantly influenced by the canopy quantum efficiency. It may be possible to obtain remotely sensed estimates of canopy quantum efficiency from satellite sensors through a correlation with chlorophyll concentrations or total nitrogen content (Waring et al. 1995). Unfortunately, assessment of canopy biochemistry requires fine-resolution spectrometry and rigorous attention to atmospheric corrections. To date, only aircraft have carried such fine-resolution spectrometers (Matson et al. 1994; Smith and Curran 1995; Martin and Aber 1997).

Conclusion

In this paper, we utilized a model that combines general physiological principles into a model that can be driven, almost entirely, from readily available monthly weather records and satellite images of changing greenness across landscapes. Minimal information is required on soils and vegetation. If detailed field-based data are available on soil drought and fertility, the model's reliability is greatly increased. Using one year's satellite data (1995) and long-term climatic means, we obtained good agreement with previously published field measurements of forest growth capacity and predawn plant water stress collected at 18 sites distributed across over the eastern Siskiyous in southwestern Oregon. This comparison indicates the potential of models, such as 3-PGS, to provide reasonable estimates of forest productive capacity across the Pacific Northwest, U.S.A.

Acknowledgments

We acknowledge Dr Joe Landsberg for helpful discussions in the use of this model. We also acknowledge Dr. Sam Goward, Dr. Phil Ryan, and Dr. Steve Running for contributions in the application of the model. Mr. Stephen Brown labored long and hard in preparing the DEM for analysis. We are grateful for comments on draft copies of the manuscript by Professor Jerry Franklin (Washington State University) and Research Assistant Professor Bev Law (Oregon State University). Part of this research (NCC) was undertaken at Department of Forest Science, Oregon State University, Corvallis, whilst on leave from CSIRO Forestry and Forest Products, Australia The research reported in this article was supported by funds from the National Aeronautics and Space Administration (NASA) Grant NAG5-7506.

References

Aber, J.D., and Federer, C.A. 1992. A generalized, lumped-parameter model of photosynthesis, evapotranspiration and net primary production in temperate and boreal ecosystems. Oecologia, **92**: 463–474.

Aber, J.D., Ollinger, S.V., Federer, C.A., Reich, P., Goulden, M.L., Kicklighter, D.W., Melillo, J.M., and Lathrop, R.G. 1995. Predicting the effects of climate change on water yield and forest production in the northeastern U.S. Clim. Res. **5**: 207–222.

Atzet, T., and Waring, R.H. 1970. Selective filtering of light by coniferous forests and minimum light energy requirements for regeneration. Can. J. Bot. **48**: 2163–2167.

Battaglia, M., and Sands, P.J. 1997. Modelling site productivity of *Eucalyptus globulus* in response to climatic and site factors. Aust. J. Plant Physiol. **24**: 831–850.

Beven, K.J., and Wood, E.F. 1983. Catchment geomorphology and the dynamics of runoff contributing areas. J. Hydrol. **65**: 139–158.

Bond, B.J., Farnsworth, B.T., Coulombe, R.A., and Winner, W.E. 1999. Foliage physiology and biochemistry in response to light gradients in conifers with varying shade tolerance. Oecologia, **120**: 183–192.

Bristow, K.L., and Campbell, G.S. 1984. On the relationship between incoming solar radiation and daily maximum and minimum temperature. Agric. For. Meteorol. **31**: 159–166.

Buffo, J., Fritschen, L., and Murphy, J. 1972. Direct solar radiation on various slopes from 0° to 60° north latitude. USDA For. Serv. Res. Pap. PNW-142.

Burrough, P.A. 1986. Principles of geographical information systems for land resources assessment. Clarendon Press, Oxford, U.K.

Coops, N.C. 2000. Comparison of topographic and physiographic properties measured on the ground with those derived from digital elevation models. Northwest Sci. **74**: 130–160.

Coops, N.C., Waring, R.H., and Landsberg, J.J. 1998*a*. Assessing forest productivity in Australia and New Zealand using a physiologically-based model driven with averaged monthly weather data and satellite derived estimates of canopy photosynthetic capacity. For. Ecol. Manage. **104**: 113–127.

Coops, N.C., Waring, R.H., and Landsberg, J.J. 1998*b*. The development of a physiological model (3-PGS) to predict forest productivity using satellite data. *In* Proceedings, Forest Scenario Modelling for Ecosystem Management at Landscape Level. *Edited by* G. Nabuurs, G.T. Nuutinen, H. Bartelink, and M. Korhonen. European Forest Institute Proc. 19. pp. 173–191.

Coops, N.C., Waring, R.H., and Landsberg, J.J. 2000*a*. Estimation of potential forest productivity across the Oregon transect using satellite data and monthly weather records. Int. J. Remote Sens. In press.

Coops, N.C., Waring, R.H., and Moncrieff, J. 2000*b*. Estimating mean monthly incident solar radiation on horizontal and inclined slopes from mean monthly temperatures extremes. Int. J. Biometeorol. In press.

Daly, C., Neilson, R.P., and Phillips, D.L. 1994. A statistical–topographic model for mapping climatological precipitation over mountainous terrain. J. Appl. Meteorol. **33**: 140–158.

Franklin, S.E., Lavigne, M.B., Deuling, M.J., Wulder, M.A., and Hunt, R., Jr., 1997. Estimation of forest leaf area index using remote sensing and GIS data for modelling net primary production. Int. J. Remote Sens. **18**: 3459–3471.

Garnier, B.J., and Ohmura, A. 1968. A method for calculating the direct shortwave radiation income on slopes. J. Appl. Meteorol. **7**: 796–800.

Gholz, H.L. 1982. Environmental limits on aboveground net primary productivity, leaf area and biomass in vegetation zones of the Pacific Northwest. Ecology, **63**: 469–481.

Goldberg, B., Klein, W.H., and McCartney, R.D. 1979. A comparison of some simple models used to predict solar irradiance on a horizontal surface. Sol. Energy, **23**: 81–83.

Goward, S.N., Tucker, C.J., and Dye, D.G. 1985. North American vegetation patterns observed with the NOAA-7 advanced very high resolution radiometer. Vegetatio, **64**: 3–14.

Goward, S.N., Waring, R.H., Dye, D.G., and Yang, J. 1994. Ecological remote sensing at OTTER: satellite macroscale observations. Ecol. Appl. **4**: 322–343.

Gower, S.T., Kucharik, C.J., and Norman, J. 1999. Direct and indirect estimation of leaf area index, *f*APAR and net primary production of terrestrial ecosystems. Remote Sens. Environ. **70**: 29–51.

Hann, D.W., and Scrivani, J.A. 1987. Dominant-height-growth and site-index equations for Douglas-fir and ponderosa pine in southwest Oregon. Forest Research Laboratory, Oregon State University, Corvallis. Res. Bull. 59.

Hungerford, R.D., Nemani, R.R., Running, S.W., and Coughlan, J.C. 1989. MTCLIM: a mountain microclimate simulation model. USDA For. Serv. Res. Pap. INT-0414.

Irwin, W.P. 1966. Geology of Klamath Mountains province. *In* Geology of northern California. *Edited by* E.H. Bailey. California Division of Mines and Geology, Sacramento. Bull. 190. pp. 19–38.

Kidwell, K.B. 1988. NOAA polar orbiter data TIROS-N, NOAA-6, NOAA-7, NOAA-8, NOAA-9, NOAA-10, NOAA-11 users guide. National Oceanic and Atmospheric Administration, Washington, D.C.

Kumar, M., and Monteith, J.L. 1982. Remote sensing of plant growth. *In* Plants and the daylight spectrum. *Edited by* H. Smith. Academic Press, London. pp. 133–144.

Landsberg, J.J. 1986. Physiological ecology of forest production. Academic Press, Sydney, Australia.

Landsberg, J.J., and Coops, N.C. 1999. Modelling forest productivity across large areas and long periods. Nat. Resour. Modell. **12**: 1–28.

Landsberg, J.J., and Gower, S.T. 1997. Applications of physiological ecology to forest management. Academic Press, San Diego, Calif.

Landsberg, J.J., and Waring, R.H. 1997. A generalized model of forest productivity using simplified concepts of radiation-use efficiency, carbon balance, and partitioning. For Ecol. Manage. **95**: 209–228.

Landsberg, J.J., Johnsen, K.H., Albaugh, T.J., Allen, H.L., and McKeand, S.E. 2001. Applying 3-PG, a simple process-based model designed to produce practical results, to data from loblolly pine experiments. For. Sci. In press.

Lange, O.L., Kapen, L., and Schulze, E.D. 1976. Water and plant life. Springer-Verlag, Berlin.

Law, B.E., Ryan, M.G., and Anthoni, P.M. 1999. Seasonal and annual respiration of a ponderosa pine ecosystem. Global Change Biol. **5**: 169–182.

Law, B.E., Waring, R.H., Anthoni, P.M., and Aber, J.D. 2000. Measurements of gross and net ecosystem productivity and water vapour exchange of a *Pinus ponderosa* ecosystem, and an evaluation of two generalized models. Global Change Biol. **6**: 155–168.

Lewis, J.D., Olszyk, D., and Tingey, D.T. 1999. Seasonal patterns of photosynthetic light response in Douglas-fir seedlings subjected to elevated atmospheric CO_2 and temperature. Tree Physiol. **19**: 243–252.

Malhi, Y., Baldocchi, D.D., and Jarvis, P.G. 1999. The carbon balance of tropical, temperate and boreal forests. Plant Cell Environ. **22**: 715–740.

Mark, D.M., and Csillag, F. 1990. The nature of boundaries on "area-class" maps. Cartographica, **27**: 65–68.

Marshall, J.D., and Waring, R.H. 1986. Comparison of methods of estimating leaf-area index in old-growth Douglas-fir. Ecology, **67**: 975–979.

Martin, M.E., and Aber, J.D. 1997. Estimating forest canopy characteristics as inputs for models of forest carbon exchange by high spectral resolution remote sensing *In* The use of remote sensing in the modelling of forest productivity. *Edited by* H.L. Gholz, K. Nakane, and H. Shimoda. Kluwer Academic Publishers, Dordrecht, the Netherlands. pp. 61–72.

Matson, P., Johnson, L., Billow, C., Miller, J., and Pu, R. 1994. Seasonal patterns and remote spectral estimation of canopy chemistry across the Oregon transect. Ecol. Appl. **4**: 280–298.

McArdle, R.E. 1961. The yield of Douglas-fir in the Pacific Northwest. U.S. Department of Agriculture, Washington D.C. Tech. Bull. 201.

Monje, O., and Bugbee, B. 1998. Adaptation to high CO_2 concentration in an optimal environment: radiation capture, canopy quantum yield and carbon use efficiency. Plant Cell Environ. **21**: 315–324.

Moore, I.D., Grayson, R.B., and Ladson, A.R. 1991. Digital terrain modelling—a review of hydrological, geomorphological and biological applications. Hydrol. Proc. **5**: 3–30.

Peterson, D.L., and Waring, R.H. 1994. Overview of the Oregon Transect Ecosystem Research Project. Ecol. Appl. **4**: 211–225.

Prince S.D., and Goward, S.M. 1995. Global primary production: a remote sensing approach. J. Biogeogr. **22**: 815–35.

Reed, K.L., and Waring, R.H. 1974. Coupling of environment to plant response: a simulation model of transpiration. Ecology, **55**: 62–72.

Running, S.W. 1994. Testing FOREST BGC ecosystem process simulations across a climatic gradient in Oregon. Ecol. Appl. **4**: 238–247.

Running, S.W., and Coughlan, J.C. 1988. A general model of forest ecosystem processes for regional applications. I. Hydrologic balance, canopy gas exchange and primary production processes. Ecol. Modell. **42**: 125–154.

Running, S.W., and Gower, S.T. 1991. FOREST-BGC, a general model of forest ecosystem processes for regional applications. II Dynamic carbon allocation and nitrogen budgets. Tree Physiol. **9**: 47–160.

Running, S.W., Justice, C.O., Salomonson, V., Hall, D., Barker, J., Kaufmann, Y.J., Strahler, A.H., Huete, A.R., Muller, J.-P., Vanderbilt, V., Wan, Z.M., Teillet, P., and Carneggie, D. 1994. Terrestrial remote sensing science and algorithms planned for EOS/MODIS. Int. J. Remote Sens. **15**: 3587–3620.

Runyon, J., Waring, R.H., Goward, S.N., and Welles, J.M. 1994. Environmental limits on net primary production and light-use efficiency across the Oregon transect. Ecol. Appl. **4**: 226–237.

Ryan, M.G., Lavigne, M.B., and Gower, S.T. 1997. Annual carbon cost of autotrophic respiration in boreal forest ecosystems in relation to species and climate. J. Geophys. Res. **102**(D24): 28 871 – 28 883.

Scholander, P.F., Hammel, H., Bradstreet, E.D., and Hemmingsen, E.A. 1965. Sap pressure in vascular plants. Science (Washington, D.C.), **148**: 339–346

Sellers, P.J. 1985. Canopy reflectance, photosynthesis and transpiration. Int. J. Remote Sens. **68**: 1335–1372.

Sellers, P.J. 1987. Canopy reflectance, photosynthesis, and transpiration 2. The role of biophysics in the linearity of their interdependence. Remote Sens. Environ. **21**: 143–183.

Singer, M.J., and Munns, D.N. 1987. Soils: an introduction. Macmillan Publishing Co., New York.

Smith, G.M., and Curran, P.J. 1995. The estimation of foliar biochemical content of a slash pine canopy from AVIRIS imagery. Can. J. Remote Sens. **21**: 234–244.

Swift, L.W. 1976. Algorithm for solar radiation on mountain slopes. Water Resour. Res. **121**: 108–112.

U.S. Department of Agriculture (USDA). 1991. State Soil Geographic Data Base (STATSGO). USDA Soil Conservation Service, Washington D.C. Misc. Publ. 1492.

Waring, R.H. 1969. Forest plants of the eastern Siskiyous: their environmental and vegetational distribution. Northwest Sci. **43**: 1–17.

Waring, R.H. 1970. Matching species to site. *In* Regeneration of ponderosa pine *Edited by* R.K. Hermann. Forest Research Laboratory, Oregon State University, Corvallis. pp. 54–61.

Waring, R.H. 2000. A process model analysis of environmental limitations on the growth of Sitka spruce plantations in Great Britain. Forestry, **75**: 65–79

Waring, R.H., and Cleary, B.D. 1967. Plant moisture stress: evaluation by pressure bomb. Science (Washington, D.C.), **155**: 1248–1254.

Waring, R.H., and Running, S.W. 1998. Forest ecosystems: analysis at multiple scales. Academic Press, San Diego, Calif.

Waring, R.H., and Youngberg, C.T. 1972. Evaluating forest sites for potential growth response of trees to fertilizer. Northwest Sci. **46**: 67–75.

Waring, R.H., Reed, K.L., and Emmingham, W.H. 1972. An environmental grid for classifying coniferous forest ecosystems. *In* Proceedings—Research on Coniferous Forest Ecosystems: First Year Progress in the Coniferous Forest Biome, US/IBP—A Symposium, 23–24 Mar. 1972, Bellingham, Wash. *Edited by* J.F. Franklin, L.J. Dempster, and R.H. Waring. U.S. Dep. Agric., PNW For. Range Exp. Stn. Portland, Oreg. U.S. Government Printing Office, Washington, D.C.

Waring, R.H., Emmingham, W.H., and Running, S.W. 1975. Environmental limits of an endemic spruce *Picea breweriana*. Can. J. Bot. **53**: 1599–1613.

Waring, R.H., Emmingham, W.H., Gholz, H.L., and Grier, C.C. 1978. Variation in maximum leaf area of coniferous forests in Oregon and its ecological significance. For. Sci. **24**: 131–140.

Waring, R.H., Law, B.E., Goulden, M.L., Bassow, S.L., McCreight, R.W., Wofsy S.C., and Bazzaz, F.A. 1995. Scaling gross ecosystem production at Harvard Forest with remote sensing: a comparison of estimates from a constrained quantum-use efficiency model and eddy correlation. Plant Cell Environ. **18**: 1201–1213.

Waring, R.H., Landsberg, J.J., and Williams, M. 1998. Net primary production of forests: a constant fraction of gross primary production? Tree Physiol. **18**: 129–134.

Whittaker, R.H. 1961. Vegetation history of the Pacific Coast States and the “central” significance of the Klamath region. Madrono, **16**: 5–23.

Zheng, D., Hunt, E.R., and Running, S.W. 1996. Comparison of available soil water capacity estimated from topography and soil series information. Landsc. Ecol. **11**: 3–14.

Zwieniecki, M.A., and Newton, M. 1994 Root distribution of 12-year-old forests at rocky sites in southwestern Oregon: effects of rock physical properties. Can. J. For. Res. **24**: 1791–1796.